Electronic Supplementary Material (ESI) for Nanoscale.
This journal is © The Royal Society of Chemistry 2017

Supporting Information for

Raman Antenna Effect from Exciton-Phonon Coupling in Organic Semiconducting Nanobelts

Mao Wang[*†], Yi Gong[†], Francesc Alzina[‡], Ondrej Svobada[‖], Belén Ballesteros[‡], Clivia M. Sotomayor Torres[‡], Senbo Xiao[†], Zhiliang Zhang[†], and Jianying He*[†]*

[†]NTNU Nanomechanical lab, Department of Structural Engineering, Norwegian University of Science and Technology (NTNU), Trondheim, 7491, Norway

[‡]Catalan Institute of Nanoscience and Nanotechnology (ICN2), CSIC and the Barcelona Institute of Science and Technology, Campus UAB, Bellaterra, Barcelona, 08193, Spain

[‖]Institute of Solid Mechanics, Mechatronics and Biomechanics, Faculty of Mechanical Engineering, Brno University of Technology, Technická 2896/2, Brno, 616 69, Czech Republic.

SI-1: The calculated atomic displacement vector diagrams corresponding to the C–H vibrations.

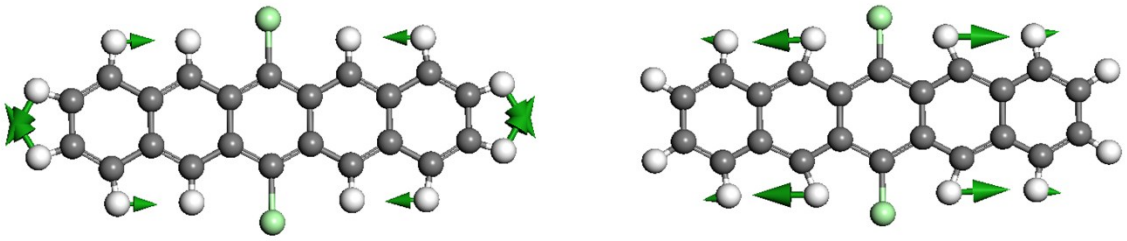

Skeletal end C–H bending
1156 cm^{-1}

Skeletal side C–H bending
1190 cm^{-1}

Figure S1. The vibration vectors diagrams correspond to the end C–H bending (the left image) and molecular skeletal side C–H bending vibrations (the right image) of DCP molecule. The gray, white and green balls in the molecular structure indicate carbon, hydrogen and chlorine atoms, respectively.

SI-2: Crystalline structure of DCP nanobelts.

The crystallographic structure of DCP single crystal has been reported in our previous results.[1] DCP crystalizes in the space group $P2_1/c$ of the monoclinic system with unit-cell dimensions of $a = 3.884$, $b = 18.718$, $c = 10.383$ Å, $\alpha = \gamma = 90.000°$ and $\beta = 94.058°$. There are on average two DCP molecules per unit cell. Different from pentacene, the existence of chlorine groups disrupts the face-to-edge arrangement, and the interaction between the two molecules in the same unit cell is very weak because of the large distance between the two molecules. DCP tends to form herringbone 1D π-π stacking along crystallographic *a*-axis, and the intermolecular distance between neighboring face-to-face

molecules is about 3.475 Å, which indicates strong π-π interaction and large transfer integral between adjacent molecules.[2, 3]

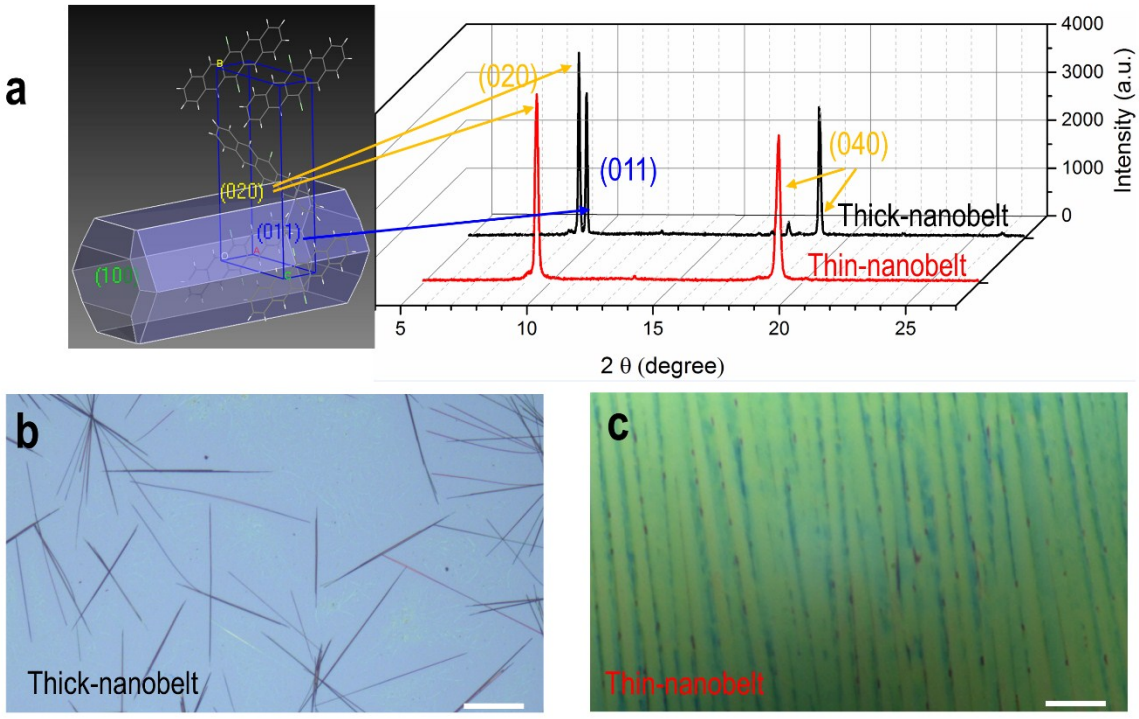

Figure S2. a) The crystal morphology modeled with BFDH method (left) and thin-film XRD patterns (right figure) of the two different kinds of DCP nanobelts. The XRD spectrum of the thin-nanobelt exhibits diffraction peaks of (020) and (040), indicating plane (020) is the top surface of the nanobelt. For the thick nanobelts, there is also a diffraction peak corresponding to plane (011), which suggests plane (011) is another main crystallographic surface for the thick nanobelts. The BFDH results show that plane (020) and (011) dominate the crystal surface, demonstrating the rationality of peak (011) in the XRD pattern. All the Raman spectra under resonant excitation are from the thin-DCP nanobelt. b) Optical microscopic image of random-arranged Thick-nanobelts obtained with

toluene as solvent. The scale bar length is 100 μm. c) Well-aligned thin-nanobelt arrays obtained with *o*-dichlorobenzene. The scale bar length is 15 μm.

We have prepared different aggregation forms of DCP, including vacuum-deposited crystalline film,[1] high-quality DCP crystalline nanobelts by physical vapor transport[4] and solution processing methods[5]. The thin-film XRD results from all the samples had similar diffraction peaks, as shown in Figure S2. So, we conclude that DCP inclined to form the herringbone 1D π–π stacking because of the strong face-to-face interaction between adjacent molecules during the self-assembly process. In the thin-film XRD spectra, the two diffraction peaks at $2\theta = 9.48°$ and $2\theta = 19.03°$ fitting well with the (020) and (040) diffraction peaks based on the single crystal XRD data, hence (020) plane was referred to as the main facet of the nanobelts. The *d*-spacing calculated from these peaks was ~9.33 Å, close to half value of the *b*-axis (18.72 Å) of the DCP unit cell.[1] It indicated that DCP molecules assembled themselves in the ordered manner with *b*-axis perpendicular and (*ac*)-plane parallel to the substrate surface. The atomic force microscope (AFM) images in Figure S3 confirmed that DCP grew with layer-by-layer mode and the thickness of one single layer was on average ~9.3 ± 0.5 Å,[5] which was nearly identical to the calculated *d*-spacing from the XRD results. Theoretical calculation based on Bravais-Friesdel-Donnay-Harker (BDFH) method showed the optimized morphology for DCP at aggregation state was one dimensional nanobelt along π–π stacking direction with plane (020) and (011) as the main surfaces (Figure S2a).[4] It agreed well with our XRD results. Another polymorph of DCP has been reported by Hatcher et al.[6] But our XRD results did not contain the diffraction peaks ($\theta = 13.50°$) corresponding to this polymorph, thus we refer that DCP here formed the aforementioned crystalline structure.

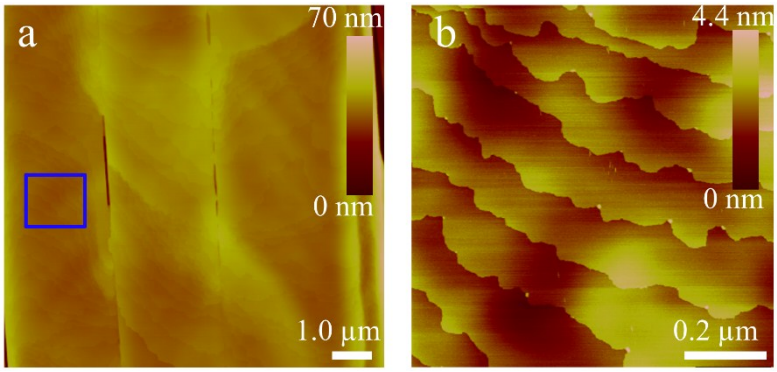

Figure S3. a) AFM image of thin-nanobelt arrays. b)[5] AFM image of the blue square in figure S3a. The top surface of DCP nanobelts was shown to be the terrace morphology with a step distance of ~9.3 ± 0.5 Å.

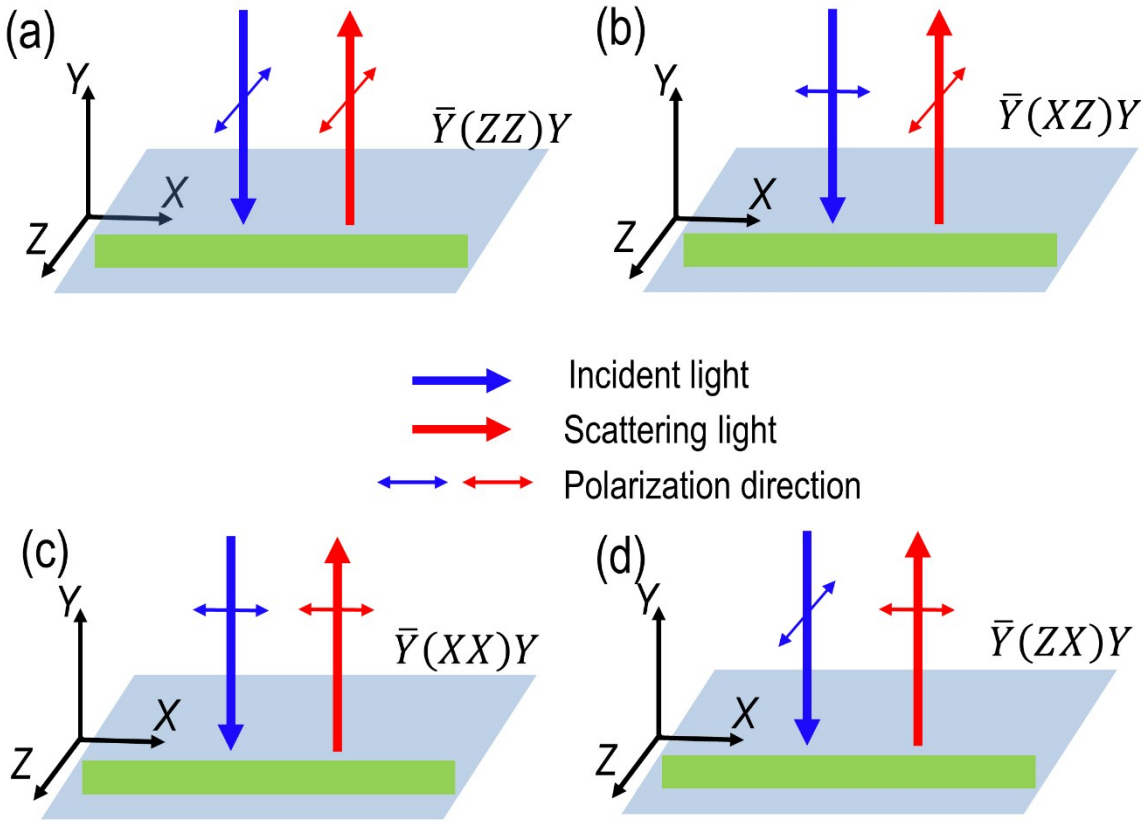

Figure S4. Schematic of the four measurement configurations adopted in our experiment, specified as (a) $\bar{Y}$(ZZ)Y ; (b) $\bar{Y}$(XZ)Y ; (c) $\bar{Y}$(XX)Y (d) $\bar{Y}$(ZX)Y in Porto notation.

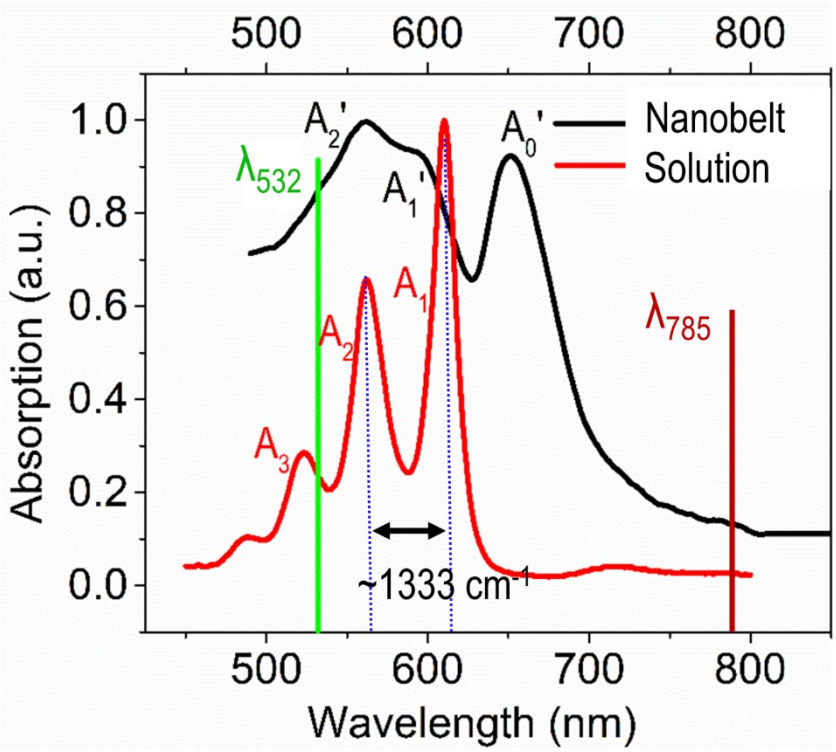

Figure S5. The absorption spectra of DCP solution in dilute chlorobenzene and DCP nanobelts. The wavelengths of excitation light at non-resonant and resonant conditions were marked as the red and green lines. For the absorption spectrum in solution, the energy distance between the two vibronic absorption peaks A_0 and A_1 was ~1333 cm^{-1}, close to the energy of vibrations along molecular short-axis.

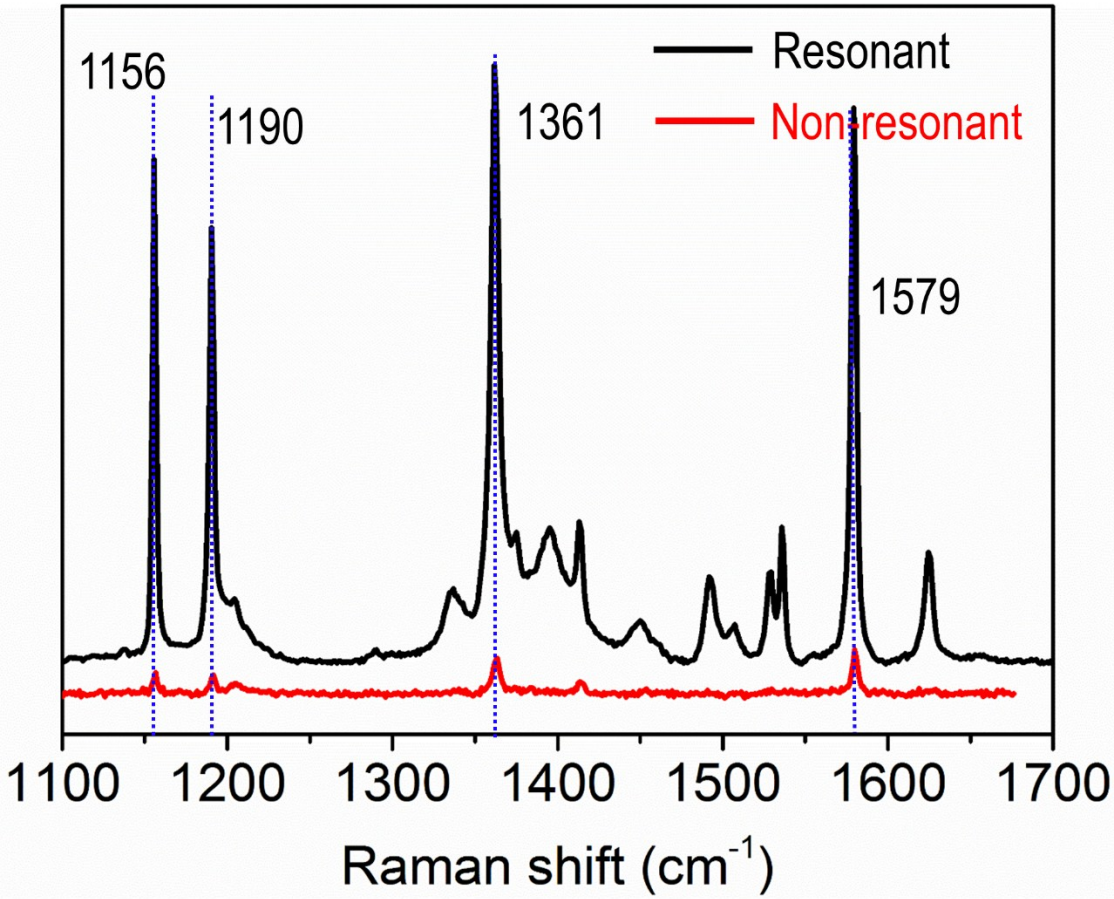

Figure S6. Comparison of the non-resonant and resonant Raman spectra of DCP nanobelts. The dotted lines indicated the four characteristic peaks discussed in the main text.

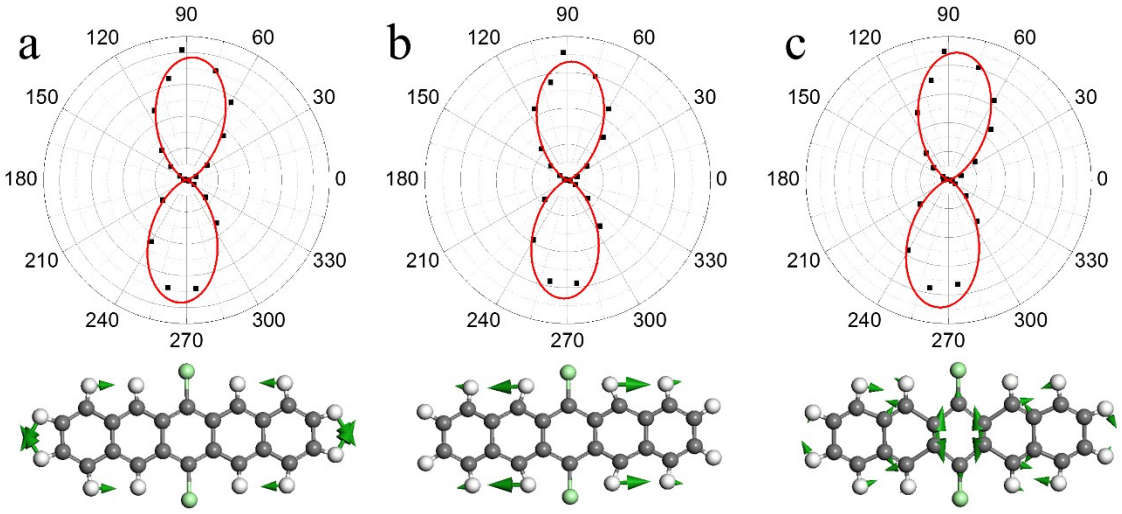

Figure S7. The up-part of each figure were polar plots of Raman intensity of corresponding peaks as a function of polarization angle (θ). The fittings function was a quartic cosine function ($I(\theta) \propto k\cos^4(\theta - \mathrm{b})$, k and b were fitting parameters). Mode 1156 cm^{-1} (a) and 1190 cm^{-1} (b) corresponded to C–H bending vibrations localized at the ends and sides of the pentacene backbone, respectively. Mode 1361 cm^{-1} (c) mainly corresponded to C–C stretching vibrations in the conjugated pentacene backbone, primarily oriented along the short-axis. θ = 0° was defined as incident light polarized parallel to the nanobelt's long-axis. All these Raman peaks showed the similar angle-dependent behavior which maximized at $\theta \approx 90°$.

Reference

1. Li, J.; Wang, M.; Ren, S.; Gao, X.; Hong, W.; Li, H.; Zhu, D. *J. Mater. Chem.* **2012,** 22, (21), 10496-10500.

2. Ostroverkhova, O. *Chem. Rev.* **2016**, 116, (2), 13279-13412.

3. Shuai, Z.; Geng, H.; Xu, W.; Liao, Y.; Andre, J.-M. *Chem. Soc. Rev.* **2014,** 43, (8), 2662-2679.

4. Wang, M.; Li, J.; Zhao, G.; Wu, Q.; Huang, Y.; Hu, W.; Gao, X.; Li, H.; Zhu, D. *Adv. Mater.* **2013,** 25, (15), 2229-2233.

5. Wang, M.; Gong, Y.; Alzina, F.; Sotomayor Torres, C. M.; Li, H.; Zhang, Z.; He, J. *J. Phys. Chem. C* **2017**, 121, (22), 12441-12446.

6. Hatcher, P. V.; Reibenspies, J. H.; Haddon, R. C.; Li, D.; Lopez, N.; Chi, X. *CrystEngComm* **2015,** 17, (22), 4172-4178.